Toughening of Polystyrene and Poly(phenylene oxide) Matrices with Elastomeric Styrene-Based Block Copolymers: Role of Molecular Architecture

INHA PARK, H. KESKKULA, and D. R. PAUL*

Department of Chemical Engineering and Center for Polymer Research, University of Texas at Austin, Austin, Texas 78712

SYNOPSIS

The effects of the molecular architecture of elastomeric styrene-based block copolymers on efficiency of toughening a brittle (polystyrene) and a ductile [a miscible blend of 80% phenylene oxide copolymer and 20% polystyrene (80PEC)] polymer were explored experimentally. Toughening appears to be mainly controlled by the blend morphology, which is determined by the rheological characteristics of the block copolymer relative to that of the matrix. The formation of dispersed particles during melt blending in a Brabender Plasticorder is strongly influenced by the ratio of the matrix and block copolymer viscosities (estimated here by Brabender torque). The size of the dispersed particles was found to be proportional to the 1.77 power of the torque ratio when this ratio is greater than unity. Thus, to a first approximation the effect of block copolymer architecture on toughening efficiency is related to how this structure affects the rheological behavior of the copolymer. Excellent toughness of polystyrene was achieved when the particle size was larger than 1–2 μm. The 80PEC resin is best toughened by block copolymers that form a cocontinuous phase morphology. The extent of toughening of this matrix appears to be a strong function of the styrene block molecular weight, whereas this structural feature seems to have no significant effect in toughening polystyrene.

INTRODUCTION

Melt blending is the simplest route to incorporation of rubber into plastics, but for simple gum rubbers this approach seldom leads to the toughening effect desired.[1-3] The reason is that effective toughening requires, at a minimum, some level of adhesive coupling between the rubber and plastic phases and a degree of control of phase morphology[1,4] usually not possible with simple elastomers. In addition, it is often desirable for the rubber phase to be crosslinked, which further limits the use of melt blending gum elastomers to achieve useful toughening of plastics. Block copolymers on the other hand can circumvent these limitations and consequently have received some attention in the literature as toughening agents for a number of plastics,[4-10] especially polystyrene (PS). Their soft segments provide the low modulus needed for the dispersed particles to act as effective stress concentrators, while their hard segments can lead to microdomains that act as physical crosslinks and can provide a mechanism of physical adhesion to the rigid matrix phase. To illustrate the latter, we would expect that a styrene-based block copolymer should adhere well to PS or to poly(phenylene oxide) (PPO), with which PS is miscible, and this has been recently demonstrated.[11-14] Based on limited information in the literature, primarily for styrene-based copolymers in a matrix of PS, the effectiveness of block copolymers as toughening agents seems to depend strongly on their molecular architecture.[6,7] The purpose here is to examine this relationship for an extensive range of block copolymer structures using matrices of PS and a material closely related to PPO. The objective is to use these as model systems to develop insight about how to design block copolymers for toughening other matrices.

* To whom all correspondence should be addressed.

Journal of Applied Polymer Science, Vol. 45, 1313–1328 (1992)
 CCC 0021-8995/92/081313-16$04.00

As mentioned earlier, phase morphology is a key issue for effective rubber toughening. It is generally believed that there is an optimum rubber particle size and that this optimum size is closely related to the nature of the postyield deformation mechanism of the matrix material that can be triggered by the rubber particles. Very brittle polymers, like PS, generally deform by multiple craze formation in the matrix[1,15-17] and require relatively large particles, of the order of several microns, to achieve optimum toughness.[8,17-21] The rubber particles must first initiate the crazes and then terminate their growth before they degenerate into cracks.[18,19,22] A growing craze may engulf rubber particles smaller than the craze thickness rather than having its growth arrested.

On the other hand, more ductile polymers like PPO, polyamides, and polycarbonate deform by shear yielding initiated at microscopically heterogeneous regions.[1,15,16,23-25] Usually, such materials require relatively smaller rubber particles for toughening than materials that craze.[17] For example, nylon 6 and nylon 6,6 are not effectively toughened unless the rubber particles are considerably smaller than 1 μm.[26-29] Wu[17,26,30] argued that interparticle distance rather than particle size is the more fundamental parameter. Recent work has shown that there is also a minimum rubber particle size for toughening nylon 6.[28] Available information[31] suggests that the optimum rubber particle size for toughening PPO is well below that for PS but probably somewhat larger than the optimum range for certain polyamides[26-29] or for styrene/acrylonitrile copolymers.[8,32] Recently, Wu[17] proposed interrelations between the molecular characteristics, the mechanisms of postyield deformation, and the optimum particle sizes for toughening of various matrix materials.

This article focuses on how the molecular architecture of styrenic block copolymers influences their efficiency for toughening PS and a miscible blend of 20 wt % PS and 80 wt % phenylene ether copolymer (PEC) that is similar in structure to PPO. This blend is designated 80PEC for convenience and is the same material used in several other recent investigations from this laboratory.[11-14] PEC is a random copolymer of 95 mol % 2,6-dimethyl phenol and 5 mol % 2,3,6-trimethyl phenol. The physical properties of PEC are similar to PPO.[33] PEC is completely miscible with polystyrene at all compositions. While polystyrene deforms by crazing, the 80PEC material primarily deforms by shear yielding.[17,25,34-36] It is of interest to compare how the toughness of blends based on these two quite different matrices respond to the molecular structure of the styrene-based block copolymers added.

EXPERIMENTAL

Materials

The PS used in this work was provided by American Petrofina Chemical Co. and is the same grade employed in several recent studies from this labora-

Table I Block Copolymers Used for Toughening of PS and 80PEC

Designation	Molecular Architecture[a]	M_n (in Thousands) Total	PS Block	Rubber	PS (%)	Source of Copolymer
X-96	S–EP	96.9	35.8	61.1	37	Shell Chemical Co.
X-97	S–EP	134.0	37.5	96.5	28	Shell Chemical Co.
X-98	30% $(S–EB)_2$	47.5	7.4	32.7	31	Shell Chemical Co.
	+ 70% S–EB	23.8	7.4	16.4	31	
X-99	S–EB–S	49.7	7.5	34.7	30	Shell Chemical Co.
X-100	20% $(S–B)_2$	111.0	17.2	76.6	31	Shell Chemical Co.
	+ 80% S–B	55.5	17.2	38.3	31	
KG 1651	S–EB–S	174.0	29.0	116.0	33.3	Shell Chemical Co.
KG 1652	S–EB–S	52.5	7.5	37.5	28.6	Shell Chemical Co.
KD 1101	S–B–S	96.5	14.5	67.5	30	Shell Chemical Co.
TRW 1601	S–EB	24.7	8.7	16.0	35.2	Shell Chemical Co.
721A	S–S/B–B–S/B–S	85.0	4.3[b]	76.5	10[b]	Firestone Rubber Co.
730A	S–S/B–B–S/B–S	140.0	21.0[b]	98.0	30[b]	Firestone Rubber Co.
840A	S–S/B–B–S/B–S	60.0	12.9[b]	34.2	43[b]	Firestone Rubber Co.

[a] S, styrene; EP, ethylene/propylene; EB, ethylene/butene-1; B, butadiene; S/B, styrene/butadiene taper.
[b] 721A, block styrene 7%; 730A, block styrene 21%; 840A, block styrene 40%.

tory.[11-14] According to the supplier, M_n = 100,000 and M_w = 350,000. The 80PEC blend was prepared for us by Borg-Warner Chemicals, Inc. by blending the polyether copolymer with the same PS mentioned above. This homogeneous blend has a T_g of 181°C.[14]

The various styrene block copolymers described in Table I were provided by the Shell Chemical Company and the Firestone Synthetic Rubber and Latex Company. Some are commercial products and their commercial designations are used. The molecular weight information shown for the commercial materials was obtained from a number of literature sources. Several experimental materials, provided by Shell, were also used. For all these materials, the soft blocks were formed from butadiene or isoprene, which in several cases were hydrogenated to obtain structures resembling copolymers of ethylene and propylene or ethylene and butene-1. Most of these materials are triblock copolymers; however, three pure diblocks are included. Two of the samples are mixtures of the coupled and uncoupled diblock materials. Coupling does not change the size of the styrene block, but it doubles the overall molecular weight and that of the diene-based block. In subsequent correlations with total copolymer molecular weight and with rubber block molecular weight, we show values for both the uncoupled and coupled species with a line drawn connecting them to emphasize the fact that these are mixtures. Alternately, one could compute average molecular weights using the percentage of each component shown in Table I. The three Firestone copolymers are commercial products designated as Stereon rubbers. These copolymers are solution-polymerized stereospecific tapered block copolymers based on butadiene and styrene. That is, there is a styrene and butadiene random copolymer region between the butadiene midblock and the styrene end blocks. Stereon 721A contains 10% by weight styrene and 3% exists in the tapered area and 7% is in the end blocks. Stereon 730A contains 30% styrene and 21% forms pure PS end blocks and 9% is in the tapered area. Stereon 840A contains 43% styrene and 40% forms pure PS end blocks while 3% is in the tapered area.[37] All polymers were dried in a vacuum oven at 60°C for 2 days prior to melt processing.

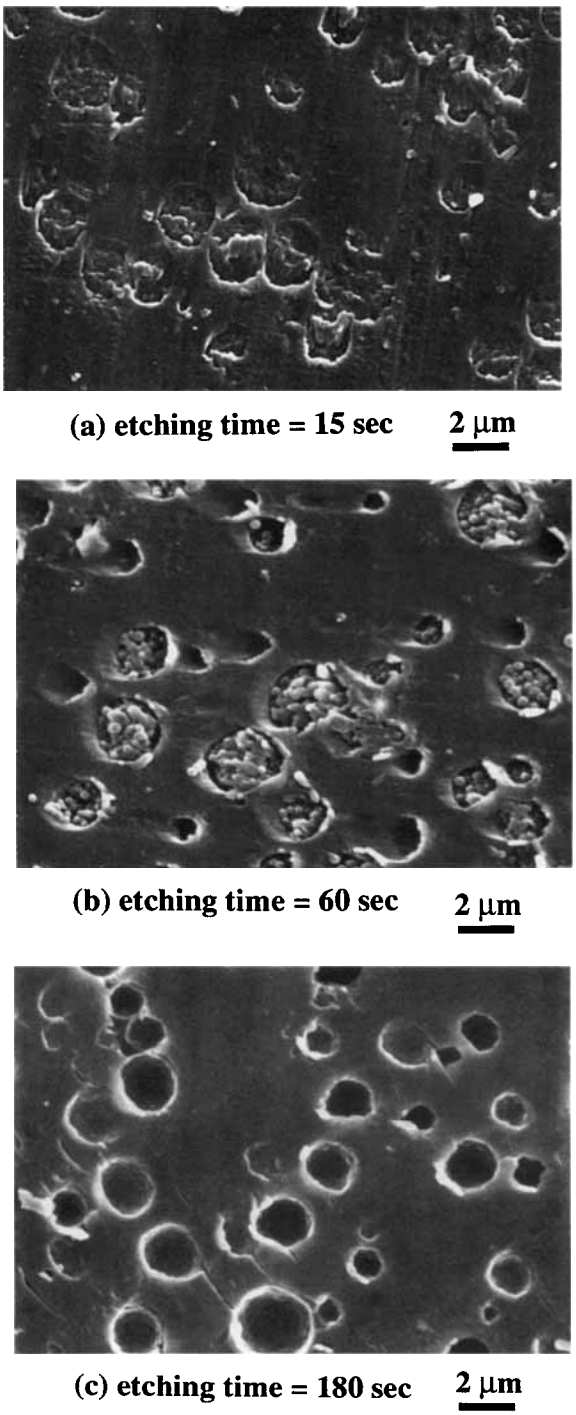

Figure 1 Scanning electron photomicrographs of HIPS etched with a mixture of chromic acid and phosphoric acid at 60°C for (a) 15 s, (b) 60 s, and (c) 180 s, respectively.

Rheological Measurements

Torque-time traces recorded from a Brabender Plasticorder with roller type blades (operated at 240°C/60 rpm for PS-based blends or at 270°C/40 rpm for 80PEC-based blends) were used for rheological characterization of the blends and their components. A steady-state torque response was usually observed about 10 min after introduction of the materials into the mixing head for most polymers ex-

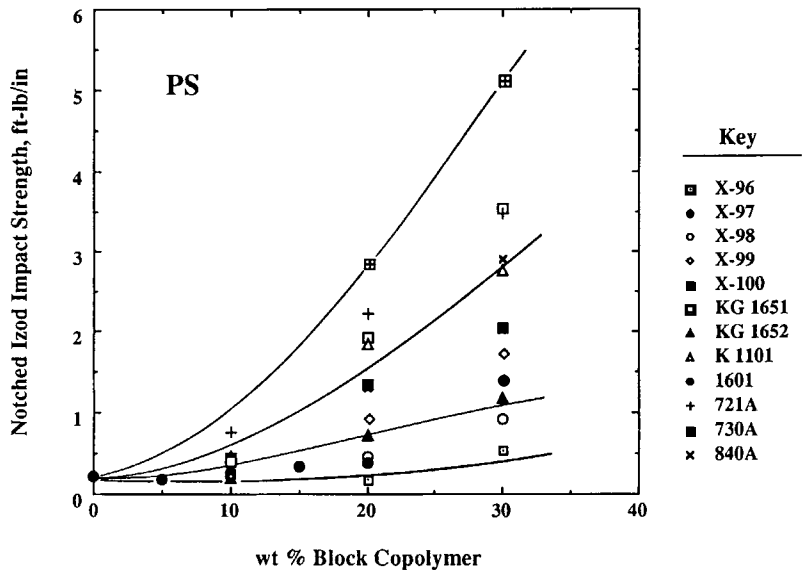

Figure 2 Notched Izod impact strength of PS-based blends with various block copolymers as a function of block copolymer content in the blends: (⊡), X-96; (♦), X-97; (○), X-98; (◇), X-99; (■), X-100; (□), KG 1651; (▲), KG 1652; (△), K 1101; (●), 1601; (+), 721A; (⊞), 730A; (×), 840A.

cept some unsaturated butadiene-based block copolymers. The torque recorded at 15 min after introduction of the materials to the mixer was used as the steady-state value for each individual polymer. To assess the sensitivity of the torque response to the amount of material in the mixing bowl, the steady-state torque responses for various polymers were examined as a function of volume of material in the mixing head. To standardize the torque measurement, the mixing bowl was filled to its nominal capacity of 60 mL. In some cases, it was necessary to force materials into the bowl to achieve this volume while for very elastic materials it was not possible to reach this limit except by extrapolation.

Blend Preparation

Test specimens were made from blends prepared in a Brabender Plasticorder. Blends of the block copolymers with PS were prepared at 240°C and 60 rpm, while the 80PEC-based blends were prepared at 270°C and 40 rpm except for those containing KG 1651. Because of the high melt viscosity of 80PEC/KG 1651 blends, a lower mixing speed of 20 rpm had to be used. To prevent oxidation during melt mixing, 0.3% Irganox B225 was added to each blend. All blends were melt mixed for a total of 15 min, after which the blends were solidified, granulated, and then compression molded into $8 \times 8 \times \frac{1}{8}$-in sheets at the same temperatures used for mixing. These sheets were cut into standard impact test bars (ASTM D-256) using a Tensilkut milling machine.

Impact Strength Measurement

Impact specimens were notched and then fractured at room temperature using a Testing Machines, Inc. impact tester. Ten specimens were tested for each blend and two values, the lowest and the highest, were discarded in calculating the average and standard deviation. The standard deviation was 5–10% of the reported values for both PS-based and 80PEC-based blends.

Morphology Analysis

Blends containing 10% block copolymer were used to obtain information about rubber phase morphology. This low level of rubber facilitated the analysis. While it is known that the size of a dispersed phase will depend on the amount of this component in the blend,[26,30,38] use of this fixed level should give an indication of differences between the various block copolymers and was necessary to limit the scope of this phase of the experimental program. Samples were microtomed at room temperature using a Reichert–Jung Ultramicrotome equipped with a glass knife to create a flat surface. Samples were then subjected to an etching solution to remove a portion of the dispersed rubber phase. The etching

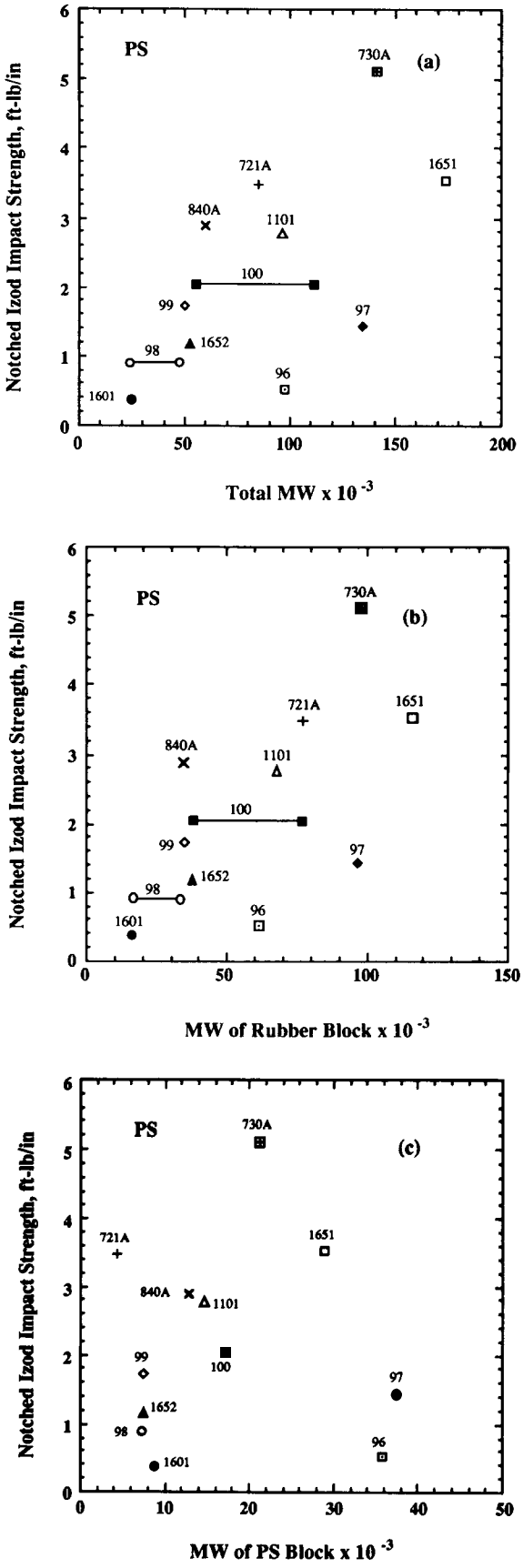

solution was a mixture of chromic and phosphoric acids prepared following the recipe reported by Bucknall et al.[39] and Hobbs[40]: 400 mL H_2SO_4, 130 mL H_3PO_4, 125 mL H_2O, and 20 g CrO_3. This approach was developed for etching unsaturated rubber; however, Yee and Diamant[7] showed it to be effective for etching a saturated rubber phase, viz., SEBS, in PS. The extent of etching depends on the temperature and time of exposure. A sample of high-impact polystyrene (HIPS) was used to examine the dependence of the observed morphology on etching conditions [see the scanning electron micrographs (SEMs) of HIPS etched for various time periods at 60°C shown in Fig. 1]. In the early stages of etching, the unsaturated rubber is selectively removed so the occluded PS in the rubber particles is clearly observed. After about 3 min, the entire rubber particle was etched away, leaving a hole such that occluded PS could not be observed. The PS matrix appeared to be quite stable against etching.

Etching conditions for the blends prepared here were carefully adjusted to obtain a shallow two-dimensional surface morphology. Sufficient etching was usually achieved in 60 s at 60°C. Etched samples were washed with water and dried in a vacuum oven for several hours at room temperature. The surface was coated with gold-palladium using a Pelco sputter coater prior to viewing in the scanning electron microscope.

A JEOL 35C scanning electron microscope equipped with a Kevex feature analyzer was operated at 25 kV to observe the morphology of the blends. The dispersed rubber particles were large enough to be observed at a magnification of 5000×. In most cases, the contrast at the particle–matrix boundary was such that the feature analyzer could not be used to correctly identify particle size. Thus, these measurements were made manually.

RESULTS AND DISCUSSION

Toughening of PS

The notched Izod impact strengths of blends with PS are shown in Figure 2 as a function of the block copolymer content in the blend. The impact strength

Figure 3 Notched Izod impact strength of PS-based blends at 30% block copolymer vs. (a) total MW of copolymer, (b) MW of rubber block, and (c) MW of PS block. Two of the materials are mixtures of a diblock copolymer and a triblock formed by coupling the diblock (see Table I). The solid lines connect the applicable molecular weights for the coupled and uncoupled molecules.

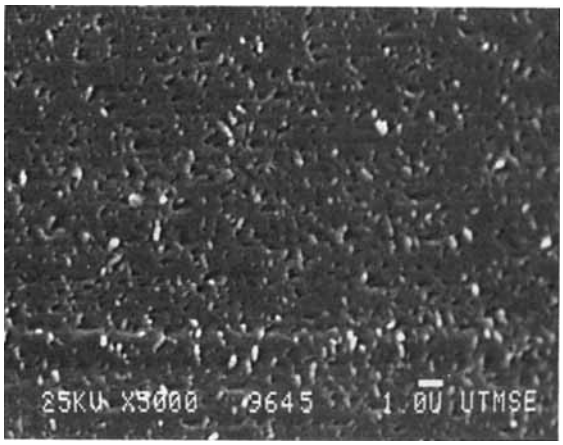

(a) 90%PS/ 10% X-96 2 μm

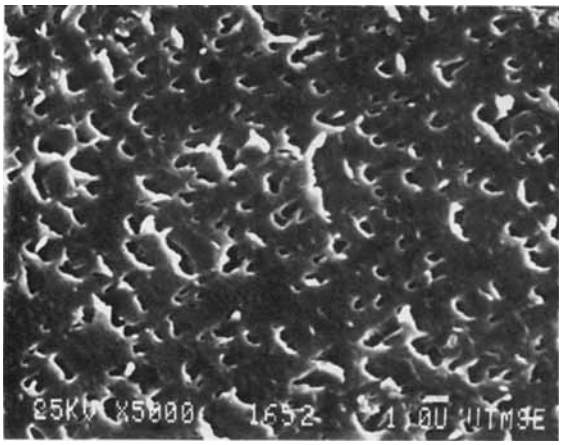

(b) 90%PS/ 10% KG 1652 2 μm

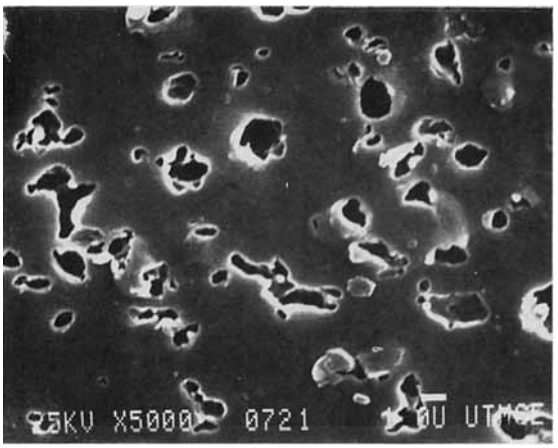

(c) 90%PS/ 10% 721A 2 μm

Figure 4 Representative scanning electron photomicrographs of PS-based blends containing 10% of various block copolymers.

increases monotonically as the block copolymer content increases for each type of block copolymer. However, the toughening efficiency depends tremendously on the block copolymer structure. To examine the origin of this effect, Izod impact strengths for blends containing 30 wt % block copolymer were interpolated from the data in Figure 2 and are plotted in Figure 3 as a function of the molecular weights of the entire copolymer, the rubber block, and the styrene block. Within this limited set of block copolymers, it is not possible to examine independently and definitively the effect of each structural variable; however, some general observations do become apparent. In Figure 3(a) and (b), it is seen that there is a general trend of increased impact strength as the total molecular weight and that of the rubber block increase. Any trend with PS block molecular weight [Fig. 3(c)] is less clear. The diblock copolymers are very inefficient impact modifiers for PS compared to the triblock copolymers. This seems to be associated with the morphology of the blends. However, the mixtures of diblock and triblock copolymers, X-98 and X-100, performed as well as the triblock copolymers. The tapered block copolymers, Stereon 730A and 840A, showed superior performance in toughening relative to all other triblock copolymers. A number of reports[6,41-43] suggest that tapered block copolymers are more effective for compatibilization of blends. This unique feature may arise from the microdomain structure it creates at the blend interface.[41-43]

Figure 4 shows representative scanning electron photomicrographs of etched surfaces of blends of polystyrene containing 10% of the various block copolymers listed in Table I. In principle, transmission electron microscopy (TEM) would give more definitive morphological information provided optimized staining conditions were used. However, this SEM-etching technique can give an adequate idea of dispersed particle size and shape with considerably less effort and skill requirement. Yee and Diamant[7] showed similar photomicrographs of Kraton KG1651 with PS that indicated PS occlusion within the rubber phase. Such features are not seen in Figure 4, and this may reflect the extent of etching at conditions selected to obtain a good definition of particle size rather than any evidence for the lack of occlusion. The rubber particles shown in Figure 4 are irregular in shape; however, an effective diameter can be assigned to each. No attempt was made to allow for the fact the microtome does not cut each particle through its equator since the usual corrections strictly apply only to spherical particles. Furthermore, etching may cause some widening of

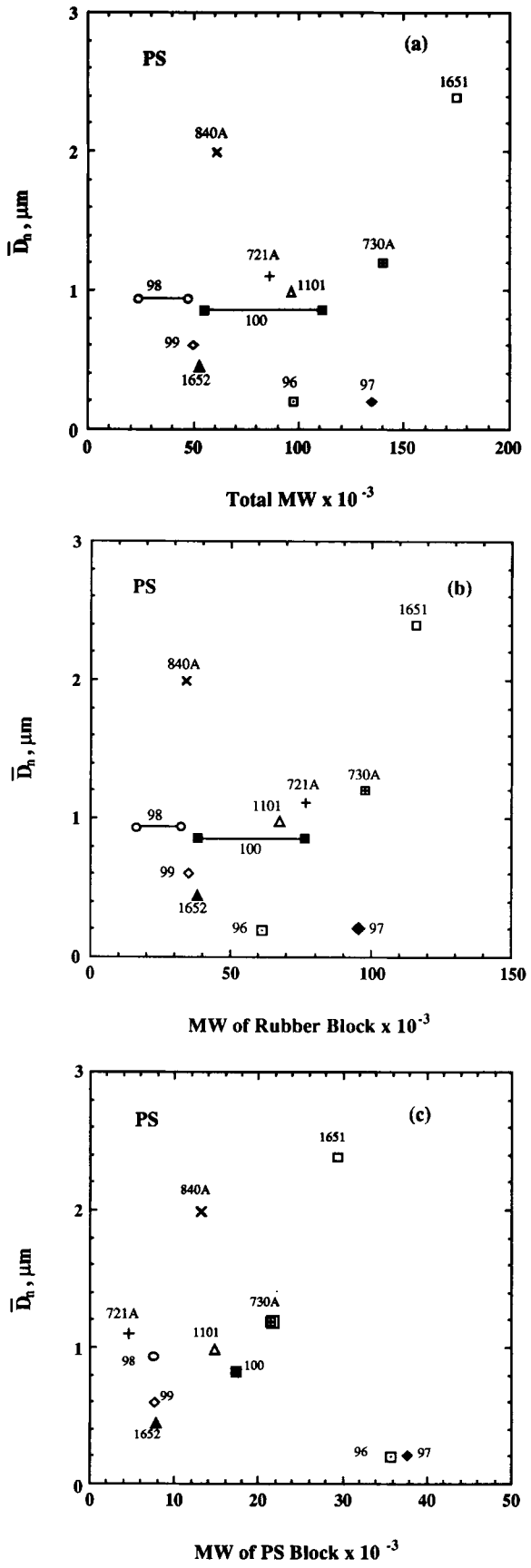

the hole when the tops of particles are cut off. From a population of 10–20 particles in each photomicrograph, the number average effective particle diameter

$$D_n = \frac{\sum D_i n_i}{\sum n_i}$$

was calculated. It should be pointed out, however, that particle sizes obtained from 10 wt % block copolymer blends may not quantitatively reflect the absolute size of particles in blends containing 30% block copolymer for which mechanical properties were determined. For example, Favis and Willis[44] showed that particle size increases as the volume fraction of the dispersed polymer increases. However, factors like viscosity that affect particle size may be expected to have a similar effect for all compositions.

Figure 5 shows a correlation between the particle size and the molecular weight of the copolymer. The particle sizes obtained vary from about 0.3–2 μm according to the molecular weight of the triblock copolymers used. The diblock copolymers formed rather small particles (about 0.2–0.3 μm in effective diameter) regardless of the molecular weight of the segments. The rubber particles' effective diameters formed by the tapered triblock copolymers were about 1.3 μm.

The observed impact strengths of the blends containing 30% block copolymer are plotted vs. particle size of the PS-based blends containing 10% block copolymer in Figure 6. In general, toughness increases more or less directly with observed rubber particle size. These results agree well with previous observations for HIPS and toughened PS using commercial styrenic triblock copolymers.[6,11,12] The materials that deviate most significantly from the correlation line shown are X-98, 730A, 840A, and KG 1651.

Toughening of 80PEC

Figure 7 shows the notched Izod impact strength of blends of 80PEC with the various block copolymers listed in Table I as a function of block copolymer content. These results differ from those for PS in several important ways. First, the absolute Izod val-

Figure 5 Number average diameter of the rubber particles in PS-based blends containing 10% of the various block copolymers as a function of (a) total MW of copolymer, (b) MW of rubber block, and (c) MW of PS block. See Fig. 3 for meaning of solid lines.

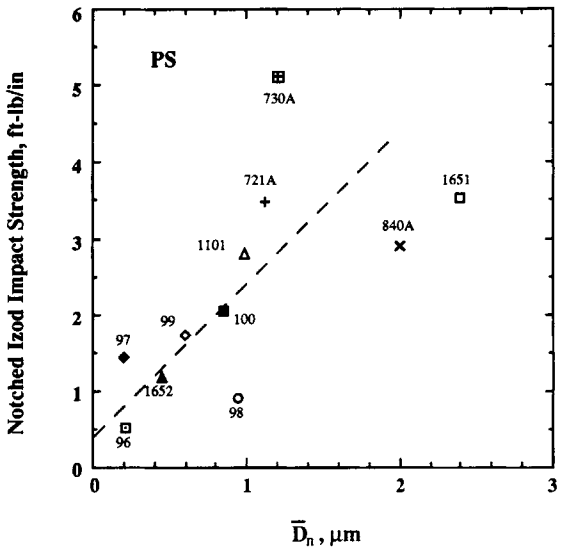

Figure 6 Notched Izod impact strength of PS-based blends containing 30% block copolymer as a function of the block copolymer domain size as given in Fig. 5.

ues rise to a higher level, 10–12 ft-lb/in, for 80PEC than PS as might be expected for a material that is inherently more ductile.[17,39] Second, the initial rate of increase of impact strength with block copolymer content is much higher for 80PEC than for PS with the result being that less elastomer is needed for toughening 80PEC than for PS. Third, in most cases the impact strength reaches a maximum and then decreases as more block copolymer is added to the 80PEC matrix. Finally, there are some major reversals in toughening efficiency for some of the block copolymers compared to PS. For example, the diblock copolymers, X-96 and X-97, that were very ineffective for toughening PS are among the most effective toughening agents for 80PEC. The tapered block copolymers, Stereon 730A and 830A, that were particularly effective for PS are not exceptional for 80PEC.

Figure 8 shows the notched Izod impact strength for 80PEC blends containing 20% block copolymer plotted vs. the molecular weight of the entire copolymer, the rubber block, and the styrene block. As with PS, there is a general trend of increasing toughness with total molecular weight and rubber block molecular weight. In contrast to PS, there also is a significant correlation between toughness and the molecular weight of the styrene block as shown in Figure 8(c). Thus, it appears that in this matrix there is a molecular role for the styrene block beyond the simple rheological one since viscosities of these block copolymers correlate only weakly at best with the size of the styrene blocks [see Fig. 13(c)]. It is worth pointing out that other recent studies have demonstrated that the styrenic microdomains of such block copolymers solubilize much greater quantities of PPO than homopolymer PS[45,46] and that these block copolymers adhere much better to PPO than to PS.[14] The fundamental reason for both

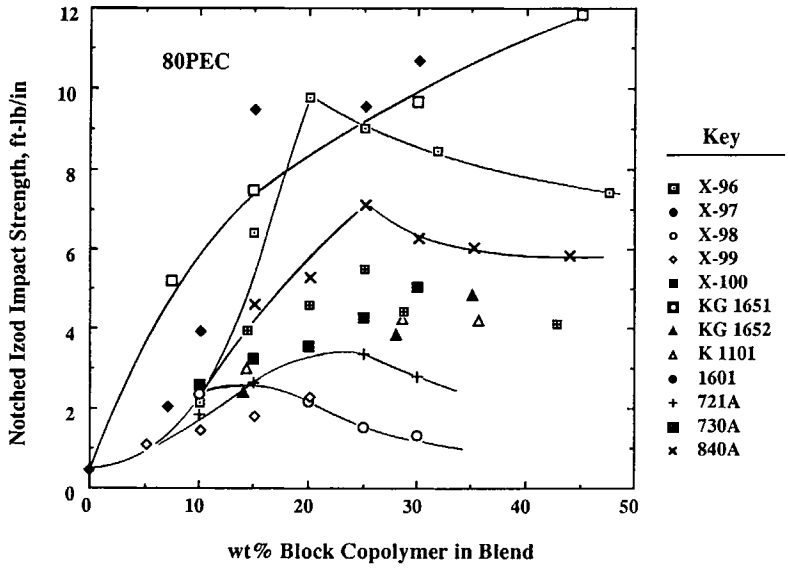

Figure 7 Notched Izod impact strength of 80PEC blends with various styrenic block copolymers as a function of block copolymer content in the blends. (⊡), X-96; (♦), X-97; (○), X-98; (◇), X-99; (■), X-100; (□), KG 1651; (▲), KG 1652; (△), K 1101; (+), 721A; (⊞), 730A; (×), 840A.

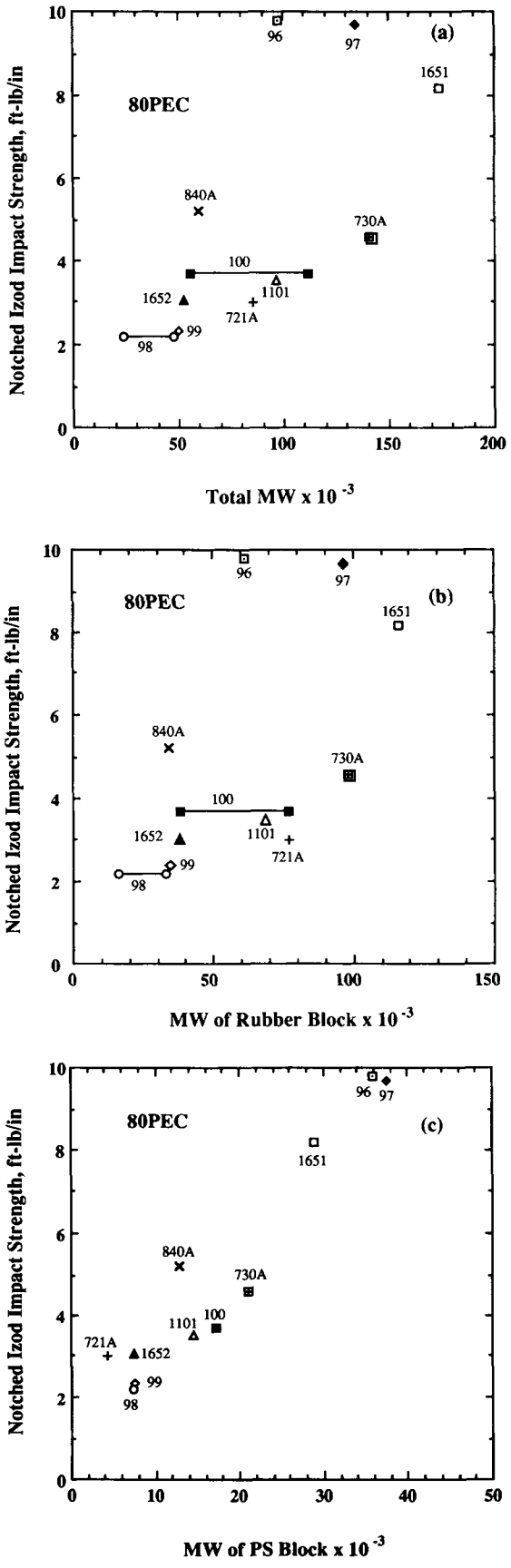

Figure 8 Notched Izod impact strength of 80PEC-based blends containing 20% block copolymer as a function of (a) total MW of copolymer, (b) MW of rubber block, and (c) MW of PS block. See Fig. 3 for meaning of solid lines.

observations relates to the strong favorable energetic interaction between PS and PPO that can drive mixing of styrene blocks with PPO whereas the only driving force for styrene blocks to mix with homopolymer PS is the very small entropy of mixing. The solubilization[45,46] and adhesion[14] mentioned above increase dramatically as the styrene block becomes longer. Consequently, we speculate that this thermodynamic issue is a factor in the correlation with styrene block length shown in Figure 8(c). One way this might manifest itself is in the morphology of the blends. The SEM procedure used here gives only a crude vision of the morphology, but it appears that the copolymers with long styrene blocks (e.g., X-96, X-97, and KG 1651), which most effectively toughen 80PEC, result in a finely dispersed, but elongated, rubber phase relative to copolymers with shorter styrene blocks (e.g., X-98 and X-99), which are less effective for toughening.

Figure 9 shows representative scanning electron photomicrographs of etched surfaces of 80PEC blends containing 10% of the various block copolymers. Even at these low contents of block copolymer, some blends tend to have a rubber-continuous morphology. Similar rubber network morphologies are apparent in the PPO domains of multicomponent blends described by Dekkers et al.[47] and Yoshimura and Richards.[48] This type of morphology may be responsible for the maximum in toughness noted for some cases in Figure 7. A true continuous phase of rubber will greatly reduce the load that can be supported and, therefore, the energy that can be dissipated during impact. It would be of interest to explore more thoroughly the mechanical properties of these blends. The blends that show the greatest level of toughness seem to be those where there is a co-continuous morphology of the 80PEC and block copolymer materials as opposed to a rubber-continuous morphology. Unlike the case with PS, it is not possible to characterize the morphology of blends based on 80PEC by an average rubber particle size since in no cases does the rubber form a simple dispersed phase. A more complete morphological analysis by TEM would be especially informative.

Rheology

It was shown above that the extent of toughening achieved by addition of elastomeric block copoly-

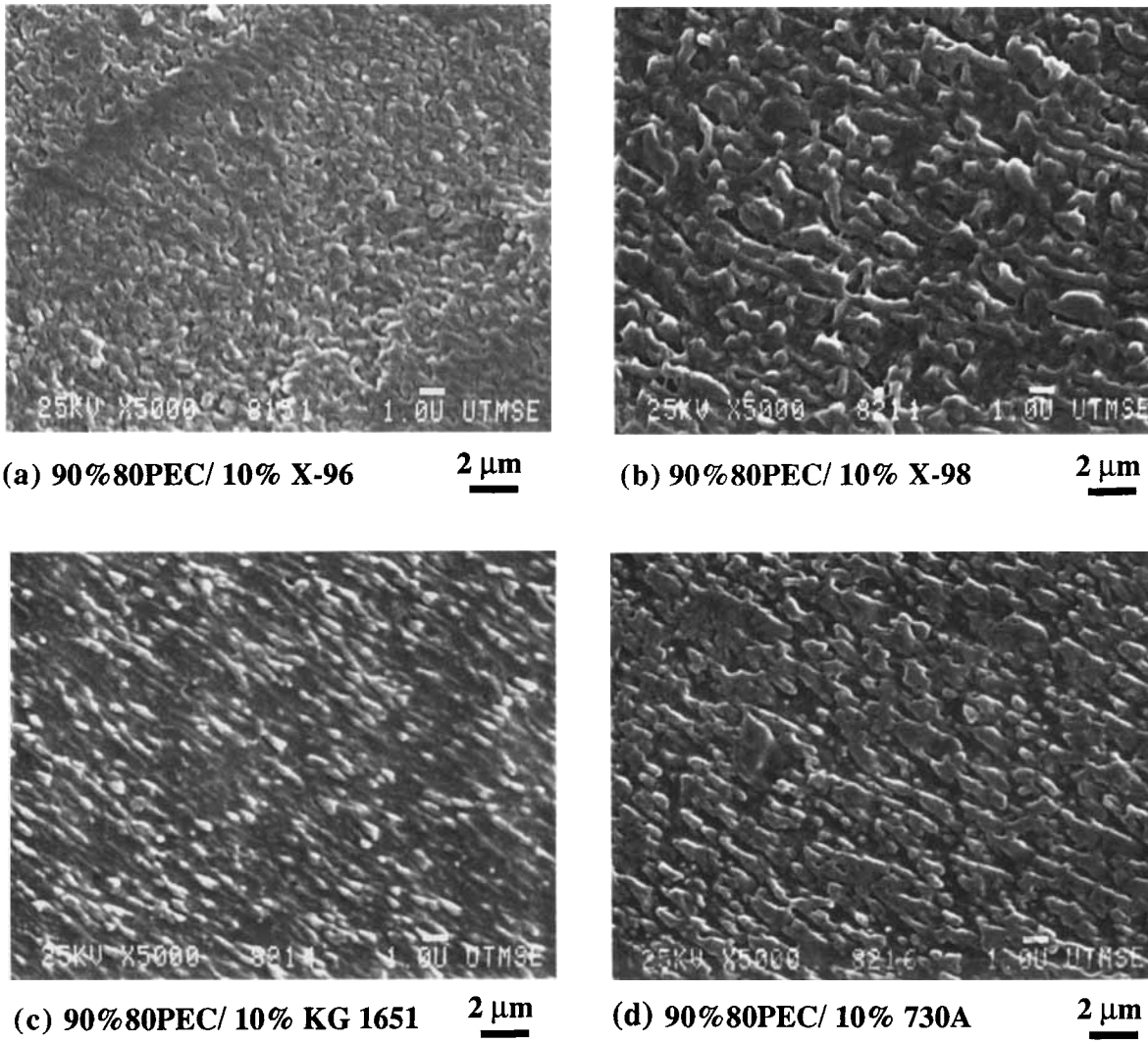

Figure 9 Representative scanning electron photomicrographs of 80PEC-based blends containing 10% of the various block copolymers.

mers is highly correlated to the morphology of the blend. In the case of the PS matrix, toughness seems to be nearly a unique function of rubber particle size for a fixed rubber content. The situation for 80PEC is more complex since the morphology cannot be characterized by a simple average phase dimension. Thus, to understand how the structural features of the block copolymer influence toughness it is necessary to understand how copolymer structure influences the morphology of the blend.

The most useful model of morphology generation during processing of immiscible blend components is to think of a balance of fluid drop break-up and phase coalescence. The final product has the morphology that is captured when the blend is solidified. The process of drop break-up can be envisioned through a model for Newtonian fluids that dates to the seminal work of Taylor.[49] Basically, a shear field will cause a drop of radius R to break up when the ratio of the surface force ($\sim\gamma/R$ where γ = interfacial tension) to the shearing force ($\sim\eta_m G$ where η_m = matrix viscosity and G = shear rate) is less than some critical ratio. The latter is a function of the ratio of the viscosity of the dispersed phase, η_d, to that of the matrix, η_m. Thus, without explicit consideration of the coalescence phenomenon, successful correlations in the form of plots of $\eta_m GR/\gamma$ vs. η_d/η_m have been constructed[50–52] for specific processing conditions. For a fixed process like that used here, i.e., a Brabender mixer operated at a constant rpm, the size of the dispersed phase becomes a function of the ratio of the viscosities of the two phases and the interfacial tension between the two components. For a fixed matrix, even η_m is no longer a

variable. In what follows, we will implicitly assume that the effective γ does not vary appreciately from one block copolymer to the other. Intuitively this seems reasonable, but in fact there is no simple alternative since such data are not available. The ultimate judge of the usefulness of this assumption will be how well the current results can be rationalized by this simple approach.

The viscosity ratio in the model can be replaced by the ratio of torque responses of the matrix and dispersed polymers[50] determined by Brabender torque rheometry. Therefore, the particle size is expected to be a function of the torque ratio of the component polymers at the processing condition, i.e.,

$$D_n = f(T_d/T_m)$$

Thus, the torque responses of the individual polymers form an essential base of information for understanding the particle size or morphology of these blends.

Figure 10 shows Brabender torque-time behavior of several representative block copolymers, PS, and 80PEC (a) at 240°C and 60 rpm and (b) at 270°C and 40 rpm. As seen in Figure 10, heating of the cold polymer and fluxing dominate the response during the first 5 min or so. After this transient, the torque begins to reflect isothermal mixing in the bowl. The steady-state torque measured after 15 min is 7.3 Nm at 240°C and 60 rpm for pure PS and 24.2 Nm at 270°C and 40 rpm for the 80PEC material. The copolymers with ethylene/propylene (EP) and ethylene/butene (EB) type saturated midblocks show a rather simple torque-time behavior. However, the copolymers with the unsaturated butadiene midblock show complicated melt behavior. The observed hump in the torque response is evidence of thermal crosslinking reactions.[53,54] The steady-state torques for the block copolymers are generally higher than that of pure PS (at 240°C and 60 rpm) but appear to be lower than that of 80PEC (at 270°C and 40 rpm).

Since the Brabender torque is very sensitive to the amount of the material in the mixing bowl, torque measurements for individual polymers must be carried out cautiously. The steady-state torques for several polymers measured after 15 min at 240°C and 60 rpm are plotted in Figure 11 as a function of the volume of the material added to the mixing head. Well-behaved thermoplastics such as PS (Fina, Cosden 550), PMMA (Rohm & Haas, V 811), and polycarbonate (GE, Lexan 131) plotted in Figure 11(a) were used to obtain an effective calibration

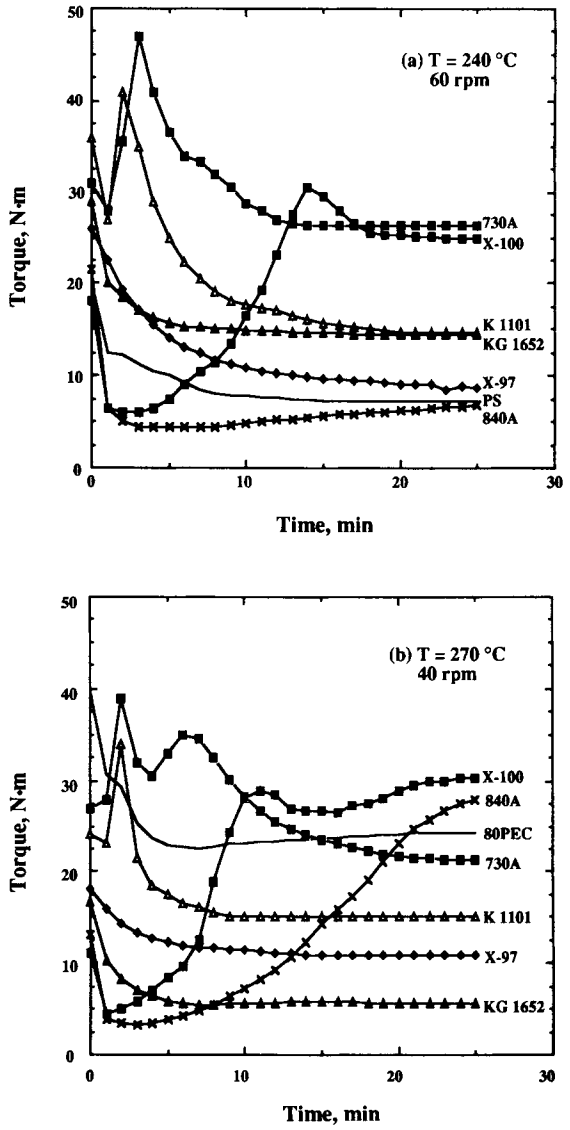

Figure 10 Brabender torque responses for PS, 80PEC, and various block copolymers at (a) 240°C and 60 rpm and (b) 270°C and 40 rpm. (♦), X-97; (■), X-100; (▲), KG 1652; (△), K 1101; (???), 730A.

of the volume of the mixing head. The nominal volume is 60 cm^3. The torque–volume relation for PC was determined at 270°C and 60 rpm because of the high viscosity of PC at 240°C. The effective volume of the mixing head appears to be about 63.4 mL. The steady-state torques for X-97, KG 1652, and 730A are plotted in Figure 11(b) as a function of volume of the material added. The torque of the butadiene-based triblock copolymer, 730A, leveled off before the mixing head was completely filled. This seems to be associated with the elasticity of the triblock copolymer due to its high molecular weight.

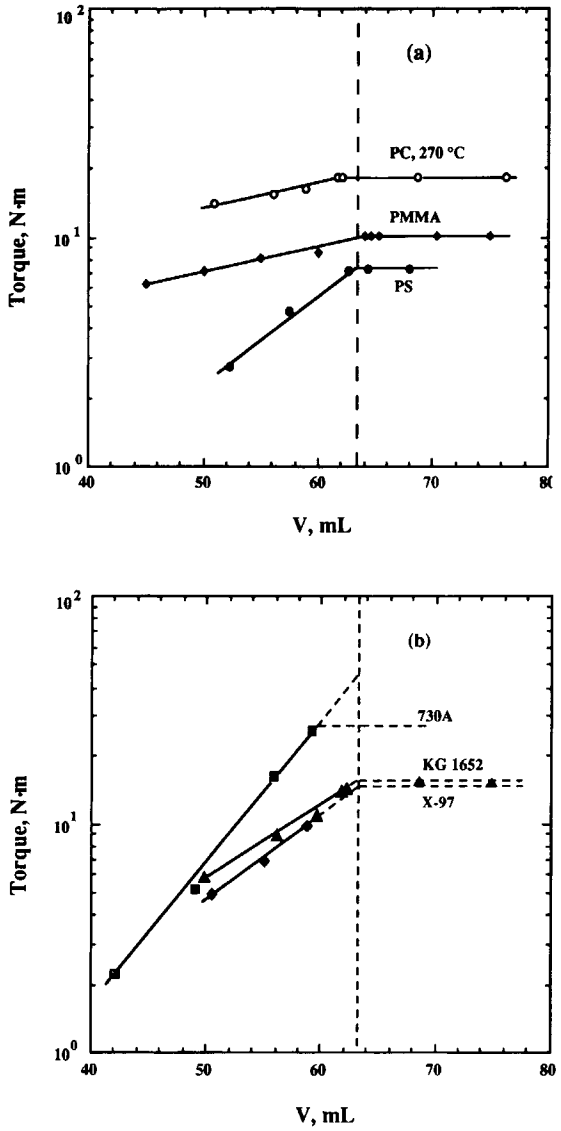

Figure 11 Steady-state Brabender torque for (a) well-behaved polymer melts and (b) highly elastic block copolymers, respectively, as a function of volume of the material added to the mixing head after 15 min at 240°C (270°C for PC) and 60 rpm.

Consequently, for such materials the torque estimated even when an excess of material is used is lower than what it should be for a completely filled mix head. Therefore, a better method to estimate the torque of such highly elastic block copolymers may be an extrapolation using data obtained at various known loadings as illustrated in Figure 11(b).

To further assess the torque behavior of the pure block copolymers, steady-state Brabender torque responses for blends with PS were measured and the results are shown in Figure 12 as a function of block copolymer composition. For most of the PS-based blends, the torque was found to be lower than the tie line. The results for blends showing somewhat abnormal torque-composition behavior are plotted in Figure 12(b). The decrease in torque at high block copolymer contents can stem from two reasons. First, the mixing head may not be completely filled with material at these high block copolymer contents due to the high elasticity of the block copolymers used. This is the case for KG 1651 and 730A. Second, the phase inversion from a PS matrix phase to a

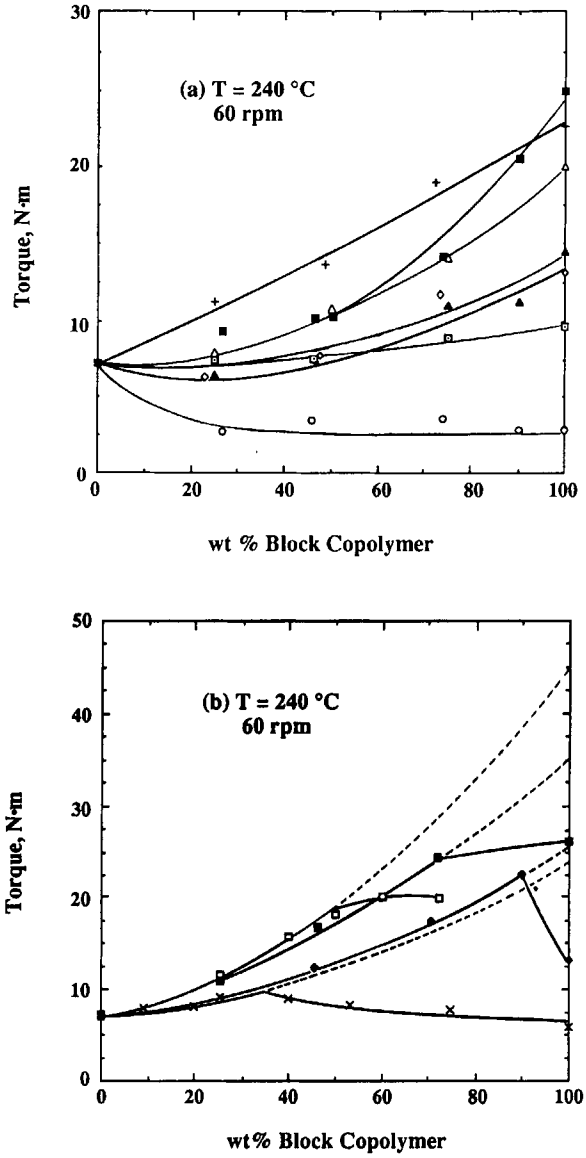

Figure 12 Brabender torque for PS-based blends with various block copolymers after 15 min at 240°C and 60 rpm: (a) blends showing normal and (b) blends showing abnormal torque-composition behavior.

rubber-continuous phase can lead to a critical torque response behavior. That is, the overall viscosity of the mixture will increase until the composition reaches the critical point and then decrease to the value of pure polymer.[51] The PS-based blends with X-97 and 840A showed this behavior. The effective torque for the four pure block copolymers mentioned above were estimated by extrapolation using the torque data measured at low block copolymer contents with a second-order polynomial regression method. The estimated and measured torque values for materials of interest here are summarized in Table II.

The torques for the pure block copolymers are plotted in Figure 13 as a function of the molecular weights of the entire copolymer, the rubber block, and the styrene block. The torques estimated by extrapolation in Figure 12(b) for the four block copolymers showing abnormal torque-composition behavior are designated with circled symbols and connected to the measured torque values with dotted lines. In general, the trend is an increase in torque as the molecular weight of the block copolymers increases. The molecular weight of the unsaturated block copolymers may increase during melt processing due to the thermal crosslinking reaction.[53,54]

In Figure 14, the number average diameter of dispersed rubber particles is plotted as a function of torque ratio for the series of PS-based blends containing 10% block copolymer prepared at 240°C and 60 rpm. The interfacial tension between the matrix PS and the rubber particles is assumed to be the same for all block copolymers. When the torque ratio is larger than unity, the following empirical correlation is obtained:

$$D_n = 0.133[(T)_{cop}/(T)_{ps}]^{1.77}$$

Wu[52] has reported similar correlations between particle size and viscosity ratio when the latter is larger than unity. The particle size seems to have a minimum at a torque ratio of unity; however, because we have only one data point below unity it is not clear if the correlation is of the V shape observed by others.[50,52] When the torque ratio is less than unity, there may be a phase inversion point based on the concentration of component polymers. The concentration of the minor component changes the shape of the curve and the location of the minimum.[50] The dispersed particles may not simply become larger as the viscosity ratio decreases below unity.

CONCLUSIONS

Several elastomeric styrene-based block copolymers were blended with a brittle and a ductile rigid polymer to determine the effect of copolymer composition and molecular architecture on efficiency for

Table II Steady State Torque for Various Block Copolymers

	Torque (Nm) at 240°C, 60 rpm		Torque (Nm) at 270°C, 40 rpm	
Designation	Measured	Estimated[a]	Measured	Estimated[a]
PS	7.3		—	
80PEC	—		23	
X-96	9.7	9.8	4.9	4.6
X-97	13.0	25.5	10.8	17.9
X-98	2.8	3.0	0.8	1.2
X-99	13.1	13.6	4.2	7.3
X-100	25.0	24.2	30.3	29.1
KG1651	[b]	44.8	[b,c]	—
KG1652	14.5	14.7	5.7	9.2
K1101	20.0	20.0	15.0	32.9
721A	22.7	22.9	24.8	63.4
730A	26.3	34.9	21.2	47.7
840A	5.6	24.0	28.0	32.7

[a] Estimated by an extrapolation using data obtained at low loadings of the block copolymers.
[b] Measurement was not able to be made since this polymer is too viscous and elastic.
[c] Blends were prepared at 270°C and 20 rpm due to the high viscosity.

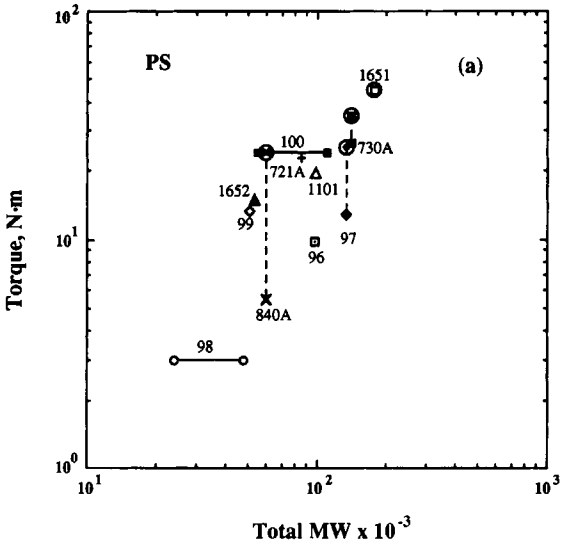

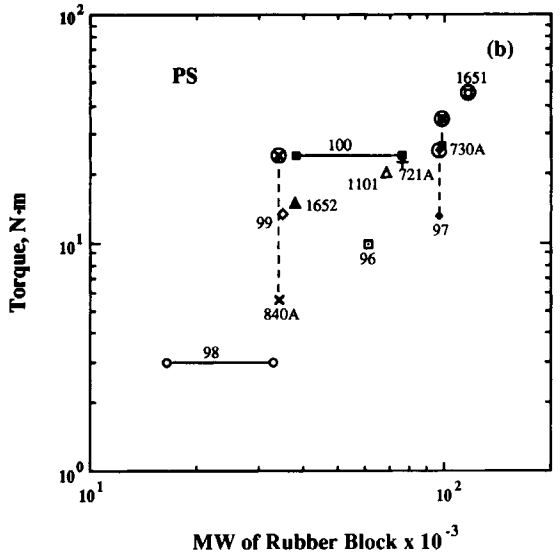

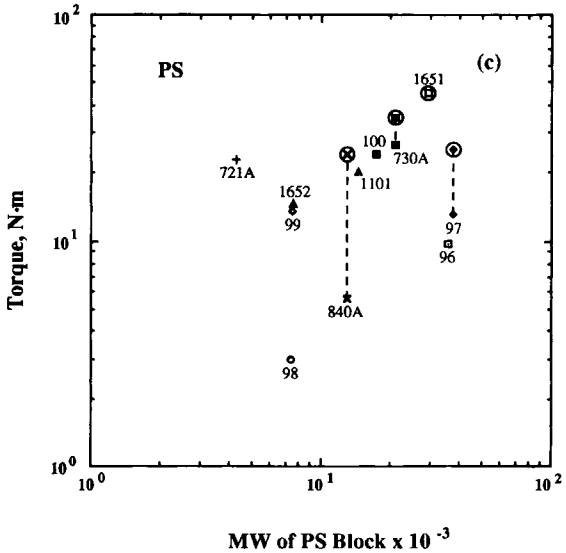

Figure 13 Brabender torque for block copolymers as a function of (a) total MW of copolymer, (b) MW of rubber block, and (c) MW of PS block. The torques estimated by extrapolation in Fig. 12(b) for the four block copolymers showing abnormal torque-composition behavior are designated with circled symbols and are connected to the measured torque values with a dotted line. See Fig. 3 for meaning of solid lines.

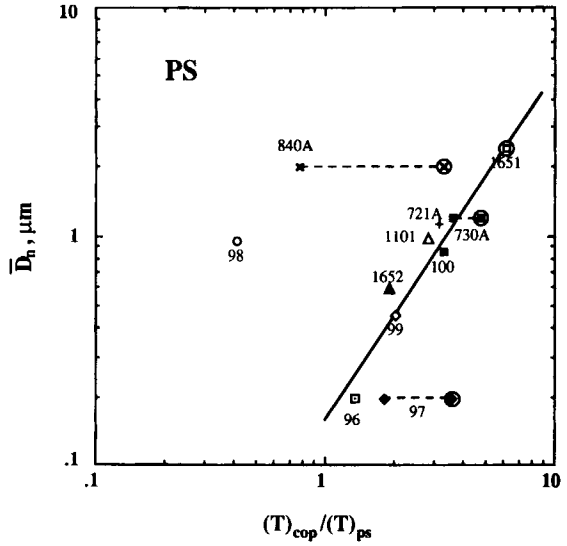

Figure 14 Number average particle diameter vs. the Brabender torque ratio for blends of block copolymers and polystyrene. See Fig. 13 for meaning of dotted lines.

toughening these matrices. As model polymers, PS and 80PEC are used for the matrix materials. The effect of molecular architecture was analyzed by correlating the Izod impact strength of PS-based blends, at a constant block copolymer content, with the molecular weights of the segments of the block copolymers. Within experimental limits, a significant correlation between the impact strength of the blend and the molecular weight of rubber block was observed for the PS-based blends. In general, the toughness of the PS-based blends increased as the rubber particles become larger; excellent toughness was achieved when the particles were of the order of 1–2 μm in diameter. Thus, the principle effect of copolymer structure is to influence the size of the dispersed rubber particles. The size of the particles is determined by the rheological properties of the copolymer relative to those of the matrix.

Toughness of the 80PEC (a miscible blend of 20% polystyrene and 80% phenylene oxide copolymer) matrix was significantly improved by addition of diblock copolymers (X-96, X-97) or a high-molecular-weight triblock copolymer (KG 1651). Beyond a

certain level of block copolymer, the notched Izod impact strength decreased as the concentration of block copolymer increased for most of the 80PEC-based blends. SEMs showed that most 80PEC/block copolymer blends had a morphology in which the elastomer was essentially a continuous phase even at 10% block copolymer. The formation of this morphology seems to stem from the fact that the melt viscosity of 80PEC is higher than that for most of the block copolymers at the blending conditions. The morphologies of the blends with excellent toughness were of a cocontinuous network type unlike the other rubber-continuous morphologies observed for most blends using low-molecular-weight triblock copolymers. Toughness seems to correlate strongly with the molecular weight of the styrene block unlike what was found for the styrene matrix case.

The toughening efficiency of the various block copolymers has been compared here on the basis of a fixed content of the entire block copolymer. Since the fraction of rubber (i.e., the midblock) varies somewhat among these copolymers, a logical alternative might be a comparison on the basis of a fixed rubber content (i.e., excluding polystyrene hard-block). This comparison is made in detail elsewhere[55] but is not shown here since none of the basic conclusions or correlations are changed from those reported in this article.

The authors express appreciation to the U.S. Army Research Office and ARCO Chemical Company for financial support. Special acknowledgment is made to Shell Chemical Company, Firestone Synthetic Rubber and Latex Company, American Petrofina Company, and Borg-Warner Chemical, Inc. for their generous supply of materials.

REFERENCES

1. C. B. Bucknall, *Toughened Plastics,* Applied Science Publishers, London, 1977.
2. R. N. Harward and J. Mann, *Proc. Roy. Soc.,* **282A,** 120 (1964).
3. H. Keskkula, S. G. Turley, and R. F. Boyer, *J. Appl. Polym. Sci.* **15,** 351 (1971).
4. H. Keskkula, in *Polymer Compatibility and Incompatibility,* Karel Solc, ed., Harwood Academic Publishers, London, 1982, pp. 323–354.
5. N. R. Legge, S. Davison, H. E. De La Mare, G. Holden, and M. K. Martin, *ACS Symp. Ser.,* **285,** 175 (1985).
6. J. R. Campbell, S. Y. Hobbs, T. J. Shea, D. J. Smith, V. H. Watkins, and I. C. W. Wang, *Contemporary Topics in Polymer Science, vol. 6, Multiphase Macromolecular Systems,* B. M. Culbertson, ed., Plenum, New York, 1990, p. 439.
7. A. F. Yee and J. Diamant, *Am. Chem. Soc., Polym. Prep.,* **9,** 92 (1978).
8. R. R. Durst, R. M. Griffith, A. J. Urbanic, and W. J. Van Essen, *Adv. Chem. Ser.,* **154,** 239 (1976).
9. A. L. Bull and G. Molden, *J. Elastom. Plast.,* **9,** 281 (1977).
10. S. L. Aggarwall, *Polymer,* **17,** 938 (1976).
11. M. C. Schwarz, J. W. Barlow, and D. R. Paul, *J. Appl. Polym. Sci.,* **35,** 2053 (1988).
12. M. C. Schwarz, J. W. Barlow, and D. R. Paul, *J. Appl. Polym. Sci.* **37,** 403 (1989).
13. M. C. Schwarz, H. Keskkula, J. W. Barlow, and D. R. Paul, *J. Appl. Polym. Sci.,* **35,** 653 (1988).
14. I. Park, J. W. Barlow, and D. R. Paul, *Polymer,* **31,** 2311 (1990).
15. I. V. Yannas and R. R. Luise, *J. Macromol. Sci.-Phys.,* **B21,** 443 (1982).
16. A. M. Donald and E. J. Kramer, *J. Mater. Sci.,* **17,** 1871 (1982).
17. S. Wu, *Polym. Engng. Sci.,* **30,** 753 (1990).
18. D. G. Gilbert and A. M. Donald, *J. Mater. Sci.,* **21,** 1819 (1986).
19. A. M. Donald and E. J. Kramer, *J. Appl. Polym. Sci.,* **27,** 3729 (1982).
20. H. Keskkula, in *Advances in Chemistry Series,* vol. 222, C. K. Riew, ed., ACS, Washington, DC, 1989.
21. H. Keskkula, M. Schwarz, and D. R. Paul, *Polymer,* **27,** 211 (1986).
22. M. Matsuo, *Polym. Engng. Sci.,* **9,** 206 (1969).
23. M. A. Maxwell and A. F. Yee, *Polym. Engng. Sci.,* **21,** 205 (1981).
24. S. T. Wellinghoff and E. Baer, *J. Appl. Polym. Sci.,* **22,** 2025 (1978).
25. C. B. Bucknall, D. Clayton, and W. E. Keast, *J. Mater. Sci.,* **7,** 1443 (1972).
26. S. Wu, *Polymer,* **26,** 1855 (1985).
27. R. J. M. Borggreve, R. J. Gaymans, and A. R. Luttmer, *Makromol. Chem., Macromol. Symp.,* **16,** 195 (1988).
28. A. J. Oshinski, H. Keskkula, and D. R. Paul, *Polymer* (to appear).
29. A. J. Oshinski, H. Keskkula, and D. R. Paul, *Polymer* (to appear).
30. S. Wu, *J. Appl. Polym. Sci.,* **35,** 549 (1988).
31. G. D. Cooper, G. F. Lee, A. Katchman, and C. P. Shank, *Mater. Tech.,* **Spring,** 12 (1981).
32. C. B. Bucknall and I. C. Drinkwater, *J. Mater. Sci.,* **8,** 1800 (1973).
33. R. I. Warren, *Polym. Engng. Sci.,* **25,** 477 (1985).
34. A. M. Serrano, G. E. Welsch, and R. Gibala, *Polym. Engng. Sci.,* **22,** 946 (1982).
35. V. F. Dalal and A. Moet, *Polym. Engng. Sci.,* **28,** 544 (1988).
36. T. A. Morelli and M. T. Takemori, *J. Mater. Sci.,* **18,** 1836 (1983).
37. Firestone Synthetic Rubber and Latex Co. product literature.
38. B. D. Favis and J. P. Chalifoux, *Polymer,* **29,** 1761 (1988).

39. C. B. Bucknall, I. C. Drinkwater, and W. E. Keast, *Polymer,* **13,** 115 (1973).
40. S. Y. Hobbs, *J. Macromol. Sci.-Rev. Macromol. Chem.,* **C19,** 221 (1980).
41. T. Hashimoto, Y. Tsukahara, and H. Kawai, *J. Polym. Sci.: Polym. Lett. Ed.,* **18,** 585 (1980).
42. Y. Tsukahara, N. Nakamura, T. Hashimoto, and H. Kawai, *Polymer J.,* **12,** 455 (1980).
43. R. Fayt, R. Jerome, and Ph. Teyssie, *J. Polym. Sci.: Polym. Phys.,* **20,** 2209 (1982).
44. B. D. Favis and J. M. Willis, *J. Polym. Sci.: Polym. Phys. Ed.,* **28,** 2259 (1990).
45. P. S. Tucker, J. W. Barlow, and D. R. Paul, *Macromolecules,* **21,** 1678 (1988).
46. P. S. Tucker, J. W. Barlow, and D. R. Paul, *Macromolecules,* **21,** 2794 (1988).
47. M. E. J. Dekkers, S. Y. Hobbs, and V. H. Watkins, *Polymer,* **32,** 2150 (1991).
48. D. K. Yoshimura and W. D. Richards, *private communication.*
49. G. J. Taylor, *Proc. Roy. Soc. (A),* **138,** 41 (1932).
50. B. D. Favis and J. P. Chalifoux, *Polym. Engng. Sci.,* **27,** 1591 (1987).
51. L. A. Utracki, *Polymer Alloys and Blends: Thermodynamics and Rheology,* Hanser Publishers, New York, 1989.
52. S. Wu, *Polym. Engng. Sci.,* **27,** 335 (1987).
53. K. McCreedy and H. Keskkula, *J. Appl. Polym. Sci.,* **22,** 999 (1978).
54. K. McCreedy and H. Keskkula, *Polymer,* **20,** 1155 (1979).
55. I. Park, PhD thesis, University of Texas at Austin, Austin, TX, 1991.

Received April 15, 1991
Accepted August 16, 1991